blood

2010 116: 2531-2542
Prepublished online June 22, 2010;
doi:10.1182/blood-2010-02-268003

Reversion of epigenetically mediated BIM silencing overcomes chemoresistance in Burkitt lymphoma

Jose A. Richter-Larrea, Eloy F. Robles, Vicente Fresquet, Elena Beltran, Antonio J. Rullan, Xabier Agirre, Maria José Calasanz, Carlos Panizo, Jose A. Richter, Jesus M. Hernandez, Jose Roman-Gomez, Felipe Prosper and Jose A. Martinez-Climent

Blood (print ISSN 0006-4971, online ISSN 1528-0020), is published weekly by the American Society of Hematology, 2021 L St, NW, Suite 900, Washington DC 20036.

Reversion of epigenetically mediated BIM silencing overcomes chemoresistance in Burkitt lymphoma

Jose A. Richter-Larrea,[1] Eloy F. Robles,[1] Vicente Fresquet,[1] Elena Beltran,[1] Antonio J. Rullan,[1] Xabier Agirre,[1] Maria José Calasanz,[2] Carlos Panizo,[3] Jose A. Richter,[4] Jesus M. Hernandez,[5] Jose Roman-Gomez,[6] Felipe Prosper,[1,3] and Jose A. Martinez-Climent[1]

[1]Division of Oncology, Center for Applied Medical Research, University of Navarra, Pamplona, Spain; [2]Department of Genetics, University of Navarra, Pamplona, Spain; [3] Hematology & Cell Therapy Programs, Clinica Universidad de Navarra, Pamplona, Spain; [4]Department of Nuclear Medicine, Clinica Universidad de Navarra, Pamplona, Spain; [5]Department of Hematology, Hospital Universitario and Center of Cancer Research, University of Salamanca-CSIC, Salamanca, Spain; and [6]Department of Hematology, Reina Sofia Hospital, Maimonides Institute for Biomedical Research, Cordoba, Spain

In Burkitt lymphoma/leukemia (BL), achievement of complete remission with first-line chemotherapy remains a challenging issue, as most patients who respond remain disease-free, whereas those refractory have few options of being rescued with salvage therapies. The mechanisms underlying BL chemoresistance and how it can be circumvented remain undetermined. We previously reported the frequent inactivation of the proapoptotic *BIM* gene in B-cell lymphomas. Here we show that *BIM* epigenetic silencing by concurrent promoter hypermethylation and deacetylation occurs frequently in primary BL samples and BL-derived cell lines. Remarkably, patients with BL with hypermethylated *BIM* presented lower complete remission rate (24% vs 79%; $P = .002$) and shorter overall survival ($P = .007$) than those with *BIM*-expressing lymphomas, indicating that *BIM* transcriptional repression may mediate tumor chemoresistance. Accordingly, by combining in vitro and in vivo studies of human BL-xenografts grown in immunodeficient RAG2$^{-/-}\gamma c^{-/-}$ mice and of murine B220^{+}IgM^{+} B-cell lymphomas generated in Eμ-*MYC* and Eμ-*MYC*-*BIM*$^{+/-}$ transgenes, we demonstrate that lymphoma chemoresistance is dictated by *BIM* gene dosage and is reversible on BIM reactivation by genetic manipulation or after treatment with histone-deacetylase inhibitors. We suggest that the combination of histone-deacetylase inhibitors and high-dose chemotherapy may overcome chemoresistance, achieve durable remission, and improve survival of patients with BL. (*Blood*. 2010;116(14):2531-2542)

Introduction

Burkitt lymphoma/leukemia (BL) is a clinically aggressive B-cell malignancy accounting for between 85% and 90% of childhood and less than 5% of adult B-cell lymphomas in Europe and the United States. Three clinical variants are recognized by the World Health Organization classification: sporadic, endemic, or related to Epstein-Barr virus (EBV) infection, and HIV-associated.[1,2] Besides the typical cytologic and immunophenotypic findings, the characteristic hallmark of BL is the presence of chromosomal translocations deregulating *MYC* oncogene.[3,4] Clinically, the presence of older age, advanced tumor stage with bone marrow and leukemic disease, increased serum lactate dehydrogenase, and immunodeficiency have been correlated with poor outcome. However, there is not a clinical or biologic marker able to predict responses to therapy.[5-10]

Current treatment for patients with BL includes multiagent, dose-intensive chemotherapy regimens with central nervous system prophylaxis, which can achieve complete remission (CR) in approximately 90% to 95% of children and 60% to 70% of adults. The most critical issue in BL remains to achieve an initial CR because those patients who respond to first-line chemotherapy have a high probability of remaining free of disease.[5,8,11] Conversely, patients who present primary chemoresistance or relapse usually die early because of progressive disease or of therapeutic complications while attempting to achieve remission.[5,12] Salvage chemotherapy has been effective in up to one-third of children with refractory or relapsed BL, but no similar successful treatment has been reported for adults.[13]

Despite this clinical issue, the molecular basis of BL chemoresistance and, more importantly, how it can be circumvented, have not been elucidated.[14-17] We have previously reported that the gene encoding the proapoptotic BH3-only family member protein BIM is frequently inactivated by genetic and epigenetic abnormalities that vary substantially among the different B-cell lymphoma subgroups.[18] In some solid tumors and myeloid leukemias, BIM is commonly inactivated by post-transcriptional modifications that target it for degradation in the proteasome, leading to therapeutic resistance.[19-23] In addition, *BIM* is a suppressor of *MYC*-induced B-cell leukemias in mice.[24,25] However, whether *BIM* mediates chemotherapeutic resistance in mature B-cell lymphomas has not been addressed. Here we show that resistance to chemotherapy in patients with BL is dictated by the epigenetic silencing of *BIM* and that this resistance can be reversed by reactivating BIM expression with histone deacetylase inhibitors (HDACis). Consequently, the combination of HDACis and high-dose chemotherapy may be of clinical benefit in patients with BL to prevent refractory disease.

Submitted February 3, 2010; accepted June 7, 2010. Prepublished online as *Blood* First Edition paper, June 22, 2010; DOI 10.1182/blood-2010-02-268003.

Presented in part as an oral communication at the 50th annual meeting of the American Society of Hematology, San Francisco, CA, December 6-9, 2008.

The online version of this article contains a data supplement.

The publication costs of this article were defrayed in part by page charge payment. Therefore, and solely to indicate this fact, this article is hereby marked "advertisement" in accordance with 18 USC section 1734.

Methods

BL primary biopsies and cell lines

Thirty-nine samples, including lymph node biopsies (n = 12) or bone marrow aspirates (n = 27) from HIV-negative Spanish patients diagnosed with BL according to the World Health Organization criteria and obtained before initiation of therapy, were included in the study. Cases with atypical BL or with Burkitt-like lymphoma were excluded (supplemental Table 1, available on the *Blood* Web site; see the Supplemental Materials link at the top of the online article). All evaluated lymphomas presented chromosomal translocations involving the *MYC* gene: t(8;14)(q24;q32) (n = 30), t(2;8)(p11;q24) (n = 2), and t(8;22)(q24;q11) (n = 3), detected by standard cytogenetics and/or fluorescence in situ hybridization.[26] All patients received standard dose-intense chemotherapy, including cyclophosphamide, anthracyclines, etoposide, vincristine, dexamethasone/prednisone, methotrexate, and cytarabine plus intrathecal prophylaxis, without rituximab therapy.[27] Clinical and follow-up data were available for 36 patients. In addition, 20 cell lines derived from patients with BL were studied, including Seraphina, Namalwa, Jijoye, Daudi, Elijah, Nab2, Raji, and EB1 (EBV^+); KHM10B, Wien133, Balm9, DG75, Ramos, BL2, BL41, CA46, Blue1, P32, and Tanoue (EBV^-); and BL5, a cell line derived from a patient with HIV-associated BL (supplemental Table 2). The study was approved by the University of Navarra Institutional Review Board, and the clinical investigation was conducted according to Declaration of Helsinki principles.

Drugs

Suberoylanilide hydroxamic acid (vorinostat), methotrexate, and dexamethasone (Merck & Co), 5-aza-2-deoxycitidine and etoposide (Sigma-Aldrich), doxorubicin and cytarabine (Pfizer), cyclophosphamide (Baxter), and vincristine (Stada) were used in the study.

Quantitative real-time RT-PCR and Western blot analyses

Measurement of the expression of *BIM* (ABI-Hs.00197982), *BAK* (ABI-Hs.00832876), and *BAX* (ABI-Hs.00180269) genes was performed with quantitative reverse-transcribed polymerase chain reaction (RT-PCR) in an ABI PRISM 7500 device (Applied Biosystems). Expression levels were normalized with *GAPDH* (ABI-Hs.99999905) as an endogenous control. Expression of BCL2 family member proteins was studied by Western blot analysis in BL cell lines, mouse lymphoma cells, and primary biopsies. The following antibodies were used: NOXA (Oncogene Research Products); BIM, BAD, BID, BAK, BAX, MCL1, and BCL2 (Stressgen); and BCL-XL (Abcam). To evaluate equal protein transfer, detection of actin protein (Oncogene Research Products) was performed. To confirm homozygous deletion of *BIM* gene locus in 2 of the BL cell lines (P32 and BL2), PCR on genomic DNA was performed according to reported methods.[18]

Methylation analysis of *BIM* promoter sequences

Detection of hypermethylation of human *BIM* gene promoter by standard methylation-specific PCR (MSP) analysis was performed as previously reported.[18] In addition, *BIM* methylation levels were measured using quantitative real-time methylation-specific PCR (quantitative RT-MSP) in a rapid fluorescent thermal cycler with 3-color fluorescence monitoring capability (LightCycler, Roche Diagnostics), using 1 μL of bisulfite-modified DNA and 1 μL of 10× LightCycler FastStar DNA Master SYBR Green I, as previously reported.[28] For pyrosequencing analysis of methylated areas, *BIM* promoter was amplified by nested PCR after bisulfite modification. Amplification products obtained in the second PCR reaction were subcloned into pCR 4-TOPO plasmid using the TOPO TA Cloning Kit for Sequencing (Invitrogen) and transformed into *Escherichia coli* according to the manufacturer's recommendations. To evaluate demethylation, BL cell lines grown at a density of 3×10^5 cells/mL in 25-cm^2 flasks with 10 mL of culture medium were treated with 2μM of the demethylating agent 5-aza-2-deoxycitidine (5-Aza) or with 2μM of the HDACi vorinostat; after incubation of 96 hours, cells were harvested for MSP, quantitative RT-PCR, and Western blot analyses.

Quantitative ChIP

BL cells were treated with 2μM of vorinostat for 48 hours and subjected to chromatin immunoprecipitation (ChIP). Quantitative PCR analysis of the ChIP fractions (10 ng) from antibody-bound and input chromatin was performed to assess the acetylated histone 3 (AcH3) modification in canonical CpG island sequences of the *BIM* promoter (AcH3; Upstate Biotechnology). SYBR Green detection was performed in the LightCycler platform (Roche Diagnostics). The amplification of the ChIP fraction and of the input DNA were used as a target and reference sequences, respectively, being amplified in the same run using BIM-ChipD (5′-AGACCTTCCCCA-GACTTGCT-3′) and BIM-ChipR (5′-TCTTTGCCCAGGACAGACTT-3′) primers. The same program conditions that for quantitative RT-MSP were applied to perform quantitative PCR-ChIP, and calculations were also performed automatically by the LightCycler software Version 2.0.[28] The level of AcH3 was determined relative to input chromatin for each sample.

MYC and *P53* gene sequencing analysis

Direct sequencing of the *MYC* gene at box I and of *P53* (exons 4-8) was performed in the ABI PRISM 3730 sequencer (Applied Biosystems), using the following primers: for *MYC* box I, forward, 5′-ACCTCGACTAC-GACTCGGTG-3′; reverse, 5′-AGAAGCCGCTCCACATACAG-3′. For *P53*, forward 5′- CTGCCGTCTTCCAGTTGC-3′; reverse 5′-TAAGCAG-CAGGAGAAAGCCC-3′ for exons 4 and 5; forward 5′-CGACAGAGC-GAGATTCCATC-3′; reverse 5′-TCCCAAAGCCAGAGAAAAGA-3′ for exon 6; forward 5′-GGTTGGGAGTAGATGGAGCC-3′; reverse 5′-CAAATGCCCCAATTGCAG-3′ for exons 7 and 8.

Ectopic transfection of *BIM* by retroviral transduction

Full-length *BIM (BCL2L11)* cDNA was cloned into the p-MIRG vector upstream from the internal ribosomal entry site of the murine stem-cell virus–internal ribosomal entry site–enhanced green fluorescent protein. p-MIRG-*BIM* and p-MIRG (empty vector) were transfected into Propack-A.52 cells (CRL-12479) obtained from ATCC using lipofectamine (Invitrogen). Then, retroviral supernatant was collected and filtered through a 0.45-μm filter. Titer of the p-MIRG-*BIM* and p-MIRG vectors was determined by infecting 3T3 cells (DSMZ) in the presence of 8 μg of polybrene (Sigma-Aldrich). For transduction of the BL cells, a 24-well plate was coated with 2 μg/mL of retronectin (Takara) at 4°C overnight. After removal of the retronectin solution, the plate was blocked for 30 minutes at room temperature with sterile phosphate-buffered saline (PBS) containing 2% bovine serum albumin. To preload the retrovirus into the plate, blocking solution was removed and 500 μL of the retroviral supernatant was added and incubated at room temperature for 1 hour. After 3 additional preload steps, 1×10^5 cells were added to each well in RPMI/10% fetal bovine serum containing 4 μg/mL of polybrene, and plates were then incubated at 37°C under 5% CO_2. Green fluorescent protein-positive cells were finally isolated using a FACSAria cell sorter (BD Biosciences). Measurement of *BIM* expression levels was performed using quantitative RT-PCR and Western blot analyses. Finally, single-cell clones were isolated from the *BIM*-expressing cell pools, and 2 of them presenting moderate and high expression levels of *BIM* (Seraphina clones 1 and 2, respectively) were selected for this study.

siRNA knockdown of BIM gene

BIM silencing was performed in 2 cell lines expressing *BIM* (KHM10B and Ramos) by transfection of 3 siRNAs (s195011, s195012, and s19474) and the Silencer Negative Control-1 siRNA (Ambion) using the Cell Line Nucleofector Solution V in a nucleofector device (Amaxa GmbH). After siRNA transfection, BIM protein expression was evaluated by Western blotting at 48 hours.

Citotoxicity and apoptosis assays

BL cells grown at a cell density of 3×10^5 cells/mL were treated with doxorubicin, vincristine, methotrexate, cytarabine, etoposide, and dexamethasone at 1, 5, 10, and 50 ng/mL, alone or in combination with 2μM vorinostat during 24 hours or with 2μM 5-Aza during 72 hours. Cell viability was assessed by trypan-blue dye exclusion. To determine apoptosis, caspase 3 and 9 activation with antibodies from BD Biosciences PharMingen and Stressgen, respectively, was used. In addition, poly(ADP-ribose) polymerase (PARP) protein expression was detected with an antibody from Promega determined using Western blot analysis. Apoptosis was also assessed by phosphatidylserine externalization using annexin V/fluorescein isothiocyanate in the presence of propidium iodide, and cell fluorescence was detected on a FACSCalibur (Becton Dickinson) using CellQuest Pro software Version 6.0, as reported.[29]

Establishment of BL xenografts in immunodeficient mice and in vivo therapy

All mouse experiments were performed in the Animal Core Facilities of Center for Applied Medical Research (University of Navarra) after approval by the local Animal Ethics Committee. To evaluate whether BL cells with different *BIM* expression levels presented variable chemotherapy resistance in vivo, 2.5×10^6 Seraphina cells transfected with p-MIRG (empty vector) or with p-MIRG-*BIM* (clones 1 and 2), and wild-type cells were intravenously injected into immunodeficient RAG2$^{-/-}\gamma c^{-/-}$ mice, which lack B, T, and NK cells.[30] Doxorubicin treatment was administered intraperitoneally on day 14 (10 mg/kg body weight) and day 21 (5 mg/kg body weight) after inoculation, whereas control mice received the corresponding vehicle (PBS). To test whether reexpression of *BIM* with vorinostat therapy in BL cells was associated with modification of sensitivity to chemotherapy in vivo, 2.5×10^6 cells from wild-type Seraphina were intravenously inoculated into RAG2$^{-/-}$IL-$\gamma c^{-/-}$ recipients. Vorinostat treatment was initiated 14 days after BL-cell inoculation and was administered intraperitoneally for 14 days (75 mg/kg body weight). Doxorubicin was administered intraperitoneally on days 14 and 21 after inoculation, 10 and 5 mg/kg body weight, respectively. In addition, cyclophosphamide was administered intraperitoneally on days 14 and 21 after inoculation (80 and 40 mg/kg body weight, respectively). Both doxorubicin and cyclophosphamide were administered alone or in combination with vorinostat. Control mice received the corresponding vehicle (dimethyl sulfoxide [DMSO]). Mouse cohorts consisted of 10 to 15 mice each, which were clinically monitored and killed when signs of tumor development were observed. To evaluate therapeutic efficacy at certain time points, mice were killed and enlarged lymph nodes and/or spleens were dissected and cell viability and apoptosis were evaluated as described above.

PET imaging of tumors in mice

To monitor tumor responses to chemotherapy in vivo, positron emission tomography (PET) imaging was performed at certain time points in a dedicated small-animal Philips Mosaic tomograph, with 2-mm resolution, 11.9-cm axial field of view, and 12.8-cm transaxial field of view. Mice were anesthetized with 2% isoflurane in 100% O_2 gas for the intravenous injection of ^{18}F-FDG (10 MBq ± 2.38 in 80-100 μL). Fifty minutes after radiotracer administration, animals were placed prone on the PET scanner bed to perform a static acquisition (sinogram) of 15 minutes under continuous anesthesia. Images were reconstructed using the three-dimensional Ramla algorithm with 2 iterations and a relaxation parameter of 0.024 into a 128 × 128 matrix with a 1-mm voxel size applying dead time, decay, and random and scattering corrections. For quantitative analysis of tumor 18 F-FDG uptake, regions of interest were drawn on coronal 1-mm-thick small-animal PET images. Regions of interest were drawn on several slices and finally, maximum standardized uptake value (SUV_{max}) was calculated for each tumor using the formula: SUV = tissue activity concentration/injected dose × body weight. SUV_{max} uptake expresses the glycolytic metabolism of tumor cells.

Lymphoma characterization, B-cell isolation, and therapy of Eμ-*MYC* and *BIM*-deficient transgenes

Eμ-*Myc* transgenic mice (C57BL/6J-Tg-IghMyc-22Bri/J) and *BIM*$^{-/-}$ knockout mice (C57BL/6J-Bcl2l11$^{tm1.1Ast}$/Bcl2l11$^{tm1.1Ast}$) were purchased from The Jackson Laboratory. Eμ-*MYC* mice were intercrossed with *BIM*$^{-/-}$ mice, and genotyping was performed to identify Eμ-*MYC*-*BIM*$^{+/-}$ mice, as reported.[24] Transgenic mice were clinically monitored and killed on overt signs of disease. Then, lymphoma cells were harvested and cell suspensions were analyzed by flow cytometry using B220 and IgM antibodies (both from BD Biosciences) to distinguish mature B-cell lymphomas (B220$^+$IgM$^+$) from pre-B-cell leukemias/lymphomas (B220$^+$IgM$^-$). To test response to chemotherapy in vitro, primary B220$^+$IgM$^+$ tumor lymphocytes were incubated in Iscove modified Dulbecco medium with inactivated fetal bovine serum, 55μM β-mercaptoethanol, and 10μg/mL anti-IgM for BCR activation. After 12 hours, cells at a concentration of $2 \times$ 49 48 ^{54} cells/mL were treated for 12 hours with doxorubicin at 0.1 μg/mL. Cell viability and apoptosis were evaluated as described in "Methods." To determine sensitivity of transgenic lymphomas to doxorubicin, 2.5×10^6 B220$^+$IgM$^+$ tumor lymphocytes obtained from Eμ-*MYC* or Eμ-*Myc*-*BIM*$^{+/-}$ mice were intravenously injected into RAG2$^{-/-}\gamma c^{-/-}$ mice (10 mice for each subgroup). One week after inoculation, doxorubicin (10 mg/kg body weight) or vehicle (PBS) was administered intraperitoneally, and tumor development was monitored in the transgenic subgroups.

Statistical analysis

To determine the statistical differences between cell viabilities, *P* values were calculated using 1-way analysis of variance test followed by Levene test to assess the homogeneity of variances (HOV). The different post hoc multiple comparison tests used were: Tukey in the case of HOV or Tamhane in the absence of HOV (for comparisons with control group), and Dunnett (for multiple comparisons). Kaplan-Meier plots were depicted to evaluate overall survival (OS) of BL patients, xenografted mouse recipients, and transgenic mice; 95% confidence interval was computed using Kalbfleish-Prentice method. Associations between individual clinical and biologic features and OS were determined using the log-rank (Mantle-Cox) test. The analyses were carried out using the SPSS 15.0 statistical software (SPSS Inc) for Windows. For comparison between median values, Fischer exact test was used.

Results

Epigenetic silencing of proapoptotic *BIM* correlates with chemoresistance in patients with BL

Our previous integrative genomic and gene expression profiling study identified frequent homozygous deletion of *BIM* gene in mantle cell lymphoma. In addition, *BIM* promoter hypermethylation was detected in germinal center-derived B-cell lymphomas, including follicular lymphoma, diffuse large B-cell lymphoma, and BL.[18] To expand this initial observation, we applied standard and quantitative MSP and pyrosequencing analyses of CpG islands of *BIM* gene promoter to BL samples, detecting *BIM* hypermethylation in 17 of 39 (46%) patient biopsies and in 15 of 18 (83%) cell lines (Figure 1A-B). Two additional BL cell lines, P32 and BL2, exhibited *BIM* gene inactivation by biallelic deletion (Figure 1C). Quantitative PCR analysis of ChIP fractions showed a decrease of AcH3 levels in canonical CpG island sequences of *BIM* promoter in hypermethylated cell lines, but not in nonmethylated tumors (Figure 1D). Concurrent *BIM* methylation and deacetylation were correlated with very low or absent RNA (Figure 1E) and protein expression levels (Figure 1F). Accordingly, treatment of methylated cells with 5-Aza or with vorinostat resulted in 1.5- to 4-fold BIM reexpression, whereas vorinostat significantly increased AcH3

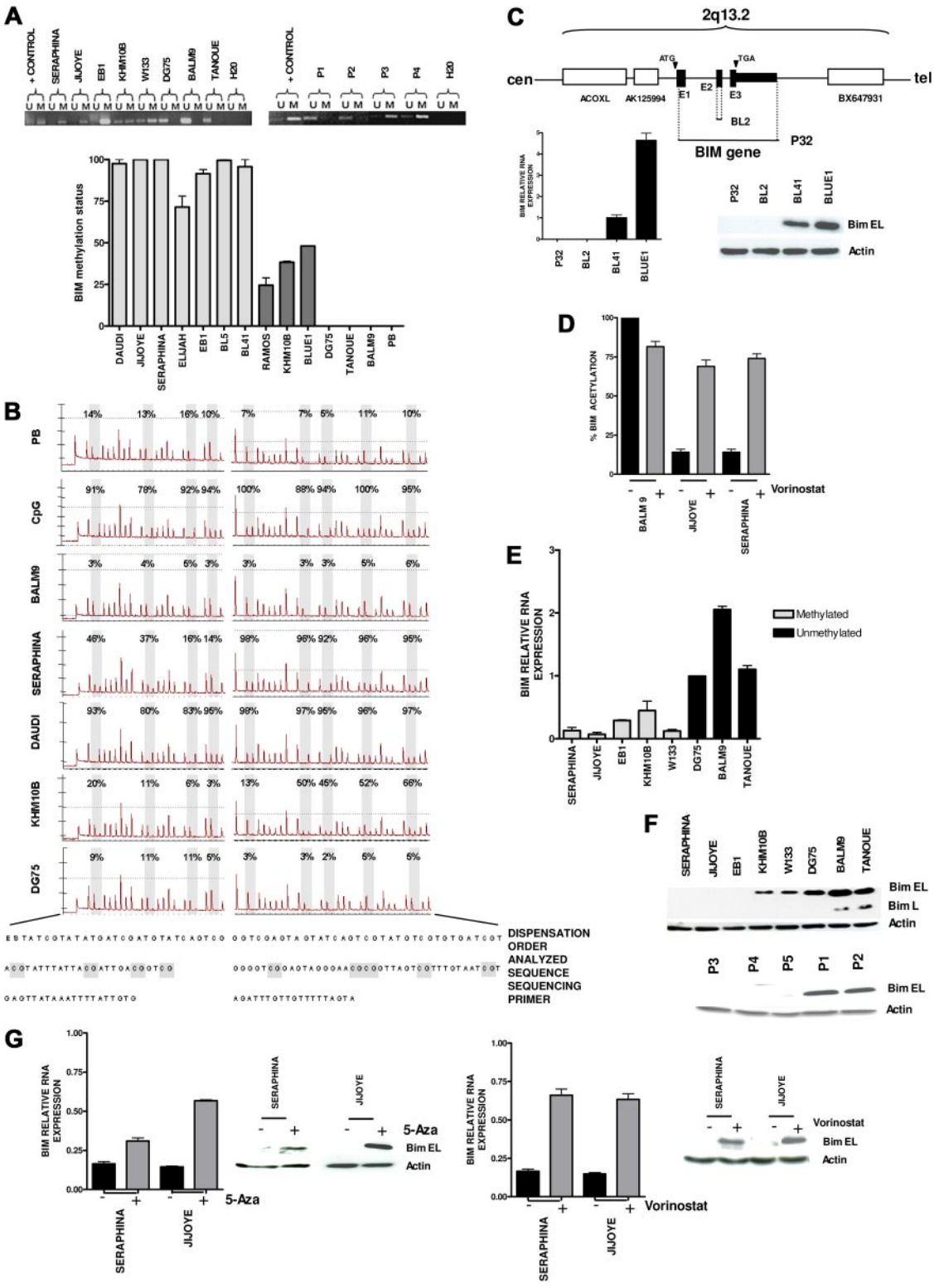

Figure 1. Epigenetic silencing of proapoptotic *BIM* gene in Burkitt lymphoma. (A) Standard MSP analysis of the *BIM* gene in BL-derived cell lines and patient samples (P1 and P2, unmethylated *BIM*; P3 and P4, methylated *BIM*; top). Quantitative analysis of methylation using quantitative MSP (bottom), including cell lines with complete methylation according to standard MSP analysis (light gray), cell lines with partial methylation (dark gray), and unmethylated tumors (DG75, Tanoue, and BALM9). PB indicates peripheral blood. (B) Pyrosequencing analysis of the *BIM* promoter area after bisulfite modification showing quantitative methylation profiles of GpG islands (expressed in percentage), which correlate with the data obtained in quantitative MSP. (C) Homozygous deletion of the *BIM* gene in the EBV- P32 and BL2 cell lines, as revealed by comparative genomic hybridization to BAC microarrays and PCR on tumor genomic DNA, resulting in null expression of BIM as shown by quantitative RT-PCR and Western blot analyses. (D) Quantitative ChIP assay of AcH3 binding to canonical CpG island sequences of *BIM* promoter in vorinostat-treated and untreated cells. An increase of AcH3 levels after treatment with vorinostat was detected in the hypermethylated Jijoye and Seraphina cell lines, but not in the unmethylated BALM9 cell line. (E) *BIM* epigenetic silencing was correlated with absent or low expression at RNA levels measured by quantitative RT-PCR, which correlate with *BIM* epigenetic status. (F) Accordingly, Western blot analysis shows protein down-regulation in BL-derived cell lines and patient samples with hypermethylation of *BIM* (P1 and P2, unmethylated *BIM*; P3, P4, and P5, methylated *BIM*). (G) Treatment with 5-Aza and with vorinostat restored BIM expression in methylated tumors at the RNA and protein levels.

Table 1. Clinical and laboratory characteristics of 36 patients with BL

	Whole series	BIM methylated	BIM unmethylated	*P*
No. (%) of patients	36	17 (47)	19 (53)	
Age, y				
Median	39	43	36	
Range	(4-76)	(6-76)	(4-68)	
Younger than 14	4 (11%)	1 (6%)	3 (16%)	.6
Sex, no. (%)				
Male	24 (67)	12 (71)	12 (63)	
Female	12 (33)	5 (29)	7 (37)	.73
Diagnosis, no. (%)				
Burkitt lymphoma	9 (25)	5 (29)	4 (21)	.71
Burkitt lymphoma-leukemia	27 (75)	13 (76)	14 (74)	
Stage III/IV, no. (%)	34 (94)	17 (100)	17 (89)	.48
Bulky disease,* no. (%)	11 (32)	4 (27)	7 (37)	.71
Extranodal involvement,* no. (%)	28 (82)	12 (80)	16 (84)	1
LDH level > 1000 IU,† no. (%)	21 (66)	9 (69)	12 (63)	1
Complete remission, no. (%)	19 (53)	4 (24)	15 (79)	.002

BL indicates Burkitt lymphoma/leukemia.
*Data are available on 34 patients.
†Data are available on 32 patients.

levels (Figure 1D,G). These data indicate that epigenetic silencing of the *BIM* gene by both hypermethylation and deacetylation occurs frequently in BL and can be pharmacologically reversed. To investigate whether *BIM* hypermethylation was correlated with clinical features, we analyzed a series of 39 Spanish patients with BL who received similar intensive chemotherapeutic regimens plus central nervous system prophylaxis.[27] Patients' clinical and laboratory data are shown in Table 1 and supplemental Table 1. All but 4 were adults, with a median age of 39 years (range, 4-76 years). The majority presented extranodal involvement (82%), including bone marrow and leukemic disease. Twenty-one of 36 patients (58%) with available clinical data achieved CR, resulting in a median OS of 15 months (95% confidence interval, 0.4-29.5; Figure 2A). *BIM* promoter hypermethylation was detected in 17 of 36 (47%) patient samples, whereas 19 cases presented the nonmethylated *BIM* gene. At diagnosis, patients with the methylated and unmethylated *BIM* were not distinguishable by the clinical and laboratory features typically associated with poor prognosis in BL (Table 1; supplemental Figure 1A). However, patients with methylated *BIM* presented lower CR rate, as only 4 of 17 cases achieved CR versus 15 of 19 patients in the unmethylated subgroup (24% vs 79%; $P = .002$). Accordingly, *BIM* hypermethylation was associated with shorter OS (median OS, 2 months vs not reached; $P = .007$; Figure 2B; supplemental Figure 1B). Similar survival data were observed for patients younger than 50 years (supplemental Figure 1C). These data indicate that *BIM* epigenetic silencing is correlated with chemotherapeutic resistance, leading to lower CR and shorter survival duration of patients with BL.

Biologic features of BL cases with *BIM* hypermethylation

We explored whether *BIM* transcriptional silencing was associated with EBV-infection status in BL cells. By quantitative MSP, higher hypermethylation levels of *BIM* gene were detected in EBV^+ lymphomas compared with EBV^- tumors (mean value, 91 ± 13 vs 35 ± 22; $P < .01$; Figure 2C). In previous reports, box I *MYC* mutations targeting Pro-57 and Thr-58 enhanced *MYC* transformation and promoted B-cell lymphoma development in mice by evading apoptosis as a result of a failure to induce *BIM*.[25,31] DNA sequencing studies revealed that box I MYC mutations spanning amino acid positions 57 to 60 were more frequent in BL cells *BIM* hypermethylation than in nonmethylated tumors (12 of 24 cases, 50% vs 6 of 16 cases, 37.5%; $P = .19$; Figure 2D; supplemental Figure 2A). Although no statistically significant values were achieved and thus no major conclusions can be drawn, these data may suggest that *MYC* mutations played a role in the epigenetic silencing of *BIM*. Next, the expression of the BCL2-family member proteins, which are critical regulators of apoptosis in B-cell malignancies, was measured by Western blot analysis in BL samples. Tumors with unmethylated *BIM* presented a higher number of alterations in the BCL2-family proteins compared with the hypermethylated cell lines (Figure 2E). BAK and BAX proteins, 2 final effectors of the apoptotic cascades, presented null or very low expression in the unmethylated cell lines while showing normal expression at the RNA level, pointing to a post-transcriptional mechanism as the putative cause of BAK/BAX down-regulation (supplemental Figure 2B). Additional studies revealed that only 2 of 9 primary hypermethylated BL biopsies showed *P53* mutation, whereas these were detected in 6 of 15 nonmethylated BL samples (22% vs 40%; $P = .24$; Figure 2F). Together, these results suggest that BIM functions as a critical regulator of apoptosis in BL cells, as its transcriptional repression is associated with a reduced number of lesions in other apoptotic regulatory proteins or in P53, indicating that *BIM* inactivation may be sufficient to evade apoptosis in BL.[24,25]

BL resistance to doxorubicin correlates with *BIM* expression levels

Patients with BL are currently treated with dose-intensive chemotherapy regimens, including cyclophosphamide, doxorubicin, vincristine, methotrexate, etoposide, dexamethasone, and cytarabine.[5,6] To test whether BIM expression was correlated with differences in cytotoxicity profiles, the Seraphina cell line, which exhibits complete *BIM* epigenetic silencing, was retrovirally transfected with a p-MIRG-*BIM* expressing vector. Two Seraphina single-cell clones with elevated BIM expression (clone 1 with a 2-fold increase, and clone 2 with a 2.5-fold increase with respect to parental cells) were selected (Figure 3A-B). Comparison of the spontaneous cell growth and apoptotic rates between the Seraphina cell clones, Seraphina cells carrying the empty vector, and wild-type cells did not show statistically significant differences (supplemental Figure 3A). Then, the lymphoma cells were incubated with the chemotherapeutic agents. A statistically significant decrease in cell viability was observed with doxorubicin, which increased cytotoxicity rates 20% to 30% in *BIM*-expressing cells compared with control cells (Figure 3A). However, these differences were not displayed with etoposide, methotrexate, cytarabine, dexamethasone, and vincristine treatment (supplemental Figure 4). We could not test cyclophosphamide in vitro, as this drug is inactive until it undergoes hepatic metabolism.[32] Treatment with doxorubicin did not increase *BIM* expression (supplemental Figure 3B) but induced cell death through the mitochondrial apoptotic pathway, as shown by activation of caspase 9 and increase of PARP (Figure 3C). Next, BIM was silenced using siRNA in the *BIM*-expressing BL cell lines Ramos and KHM10B, which were then incubated with the chemotherapeutic agents. After doxorubicin treatment, cell viability was increased along with a decrease in apoptotic rates ($\sim$ 30%–40%) in *BIM*-silenced cells compared with control cells (Figure 3D). These data indicate that selective resistance of BL cells to doxorubicin is conditioned, at least in part, by *BIM* expression levels. To test whether similar results could be observed

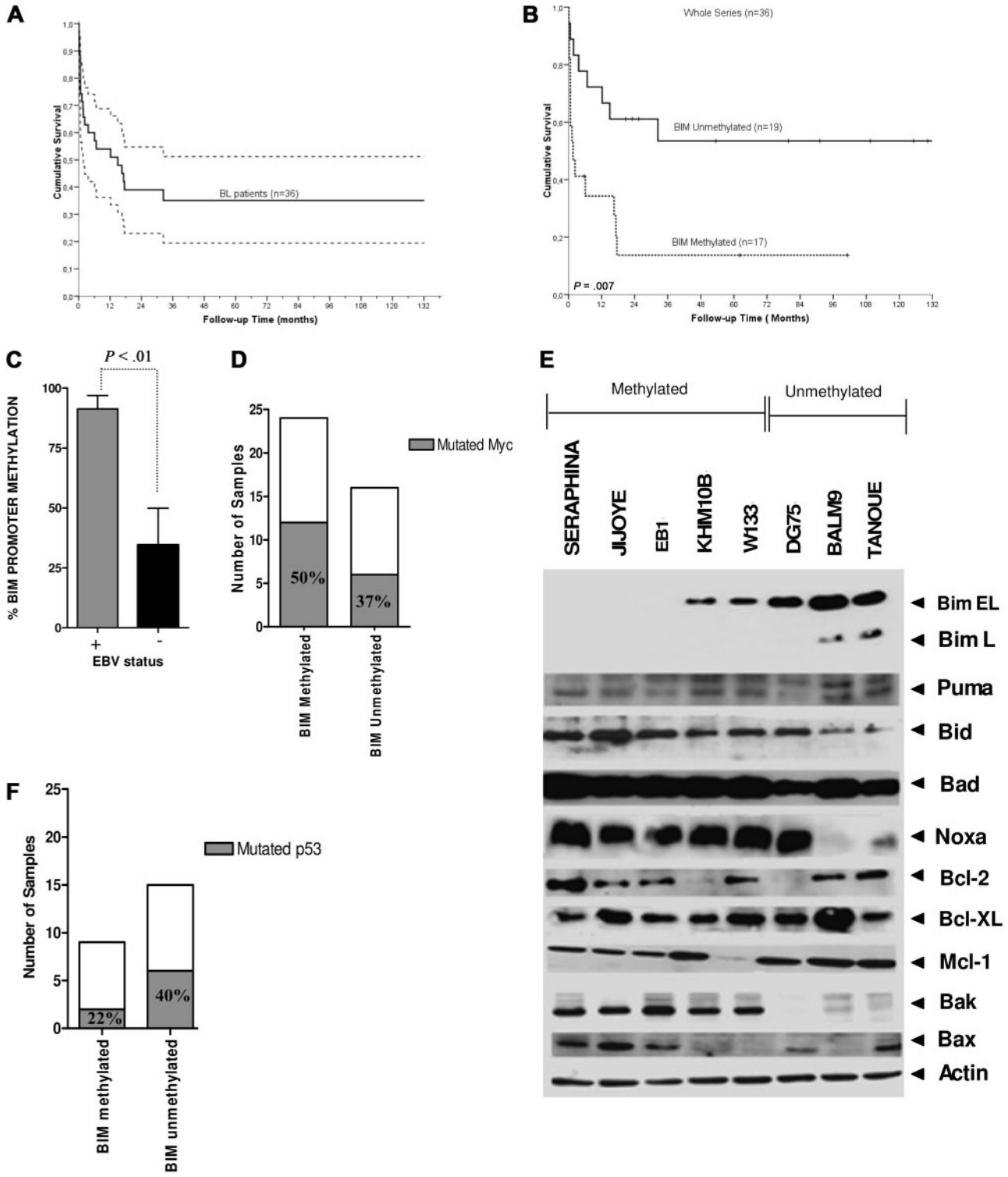

Figure 2. Correlation of *BIM* epigenetic silencing with clinical outcome and with biologic features in BL. Kaplan-Meier curves for OS for (A) 36 patients with BL included in the study and (B) BL patients with methylated and unmethylated *BIM*, where *BIM* promoter hypermethylation was correlated with inferior CR rate ($P = .002$) and shorter survival duration ($P = .007$). (C) By MSP analysis, *BIM* hypermethylation was observed in 8 EBV^+ BL cell lines and in 6 of 9 (66%) EBV-BL cell lines. By quantitative MSP analysis, measurement of *BIM* promoter hypermethylation according to EBV infection revealed higher hypermethylation levels in EBV^+ lymphomas compared with EBV^- tumors ($P < .01$). (D) Correlation of box I *MYC* mutations in BL primary samples and cell lines with and without hypermethylation of *BIM*: mutations at box I from amino acid positions 57 to 60 (including Pro-57 and Thr-58 sites) were more frequent in BL cell lines and primary samples with *BIM* hypermethylation than in nonmethylated tumors (12 of 24 cases, 50% vs 6 of 16 cases, 37.5%; $P = .19$). (E) Western blot analysis of BCL2 family proteins in BL cell lines, classified in methylated and unmethylated *BIM* subgroups. β-Actin served as loading control. (F) Sequencing of *P53* gene identified a lower number of mutations in patient samples with hypermethylated *BIM* with respect to unmethylated samples. Because almost all BL cell lines carried the *P53* mutations, this analysis was restricted to primary tumors.

in vivo, Seraphina clones 1 and 2 were intravenously inoculated into $RAG2^{-/-}\gamma c^{-/-}$ mice, which received doxorubicin or vehicle treatments. Mice carrying wild-type cells or cells transfected with the empty vector did not show differences in OS between treated

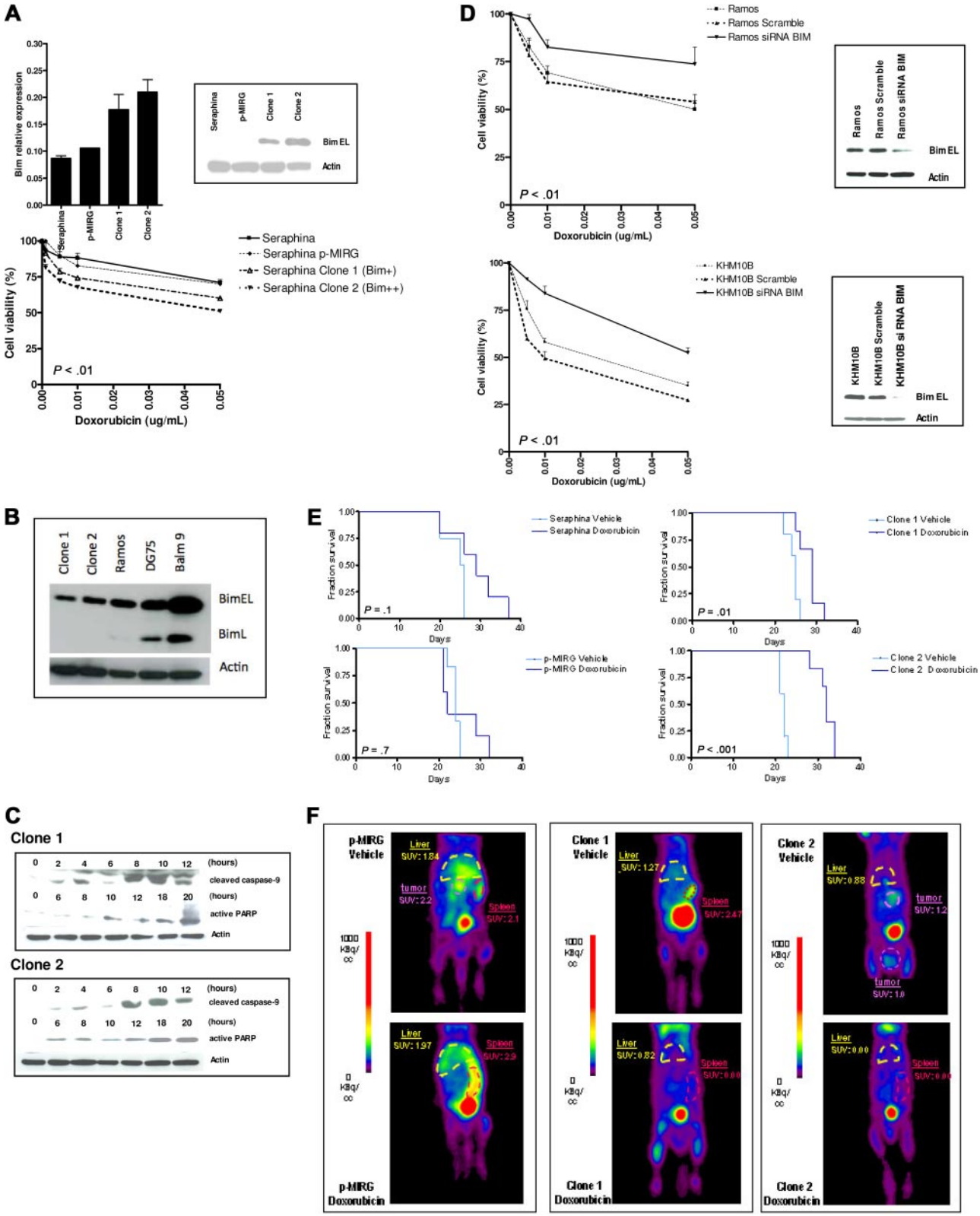

Figure 3. Correlation of BIM expression levels with chemotherapy-induced apoptosis. (A) Seraphina cells were retrovirally transfected with p-MIRG-BIM and p-MIRG (empty vector). Single-cell clones were isolated from the BIM-expressing cell pools. Using quantitative RT-PCR and Western blot analyses, clones 1 and 2 showed intermediate and high BIM expression, respectively, with respect to the parental cell line. Seraphina clones 1 and 2 were incubated with individual chemotherapeutic agents, showing increased sensitivity to doxorubicin with respect to control cells, but not to other compounds tested (supplemental Figure 4). (B) Relative BIM expression of Seraphina clones 1 and 2 and other BL cell lines. (C) Chemotherapy treatment of clones 1 and 2 cells activated the intrinsic apoptotic pathway, through cleavage of caspase 9 and expression of PARP proteins, as determined by Western blot analysis. (D) Silencing of BIM by RNA interference in Ramos and KHM10B cell lines was correlated with an increase in the resistance profile to doxorubicin with respect to parental cell line and control (cells transfected with a scramble vector). (E) Kaplan-Meier survival curves of RAG2$^{-/-}\gamma c^{-/-}$ mice transplanted with wild-type and genetically manipulated Seraphina cells, which received chemotherapy or vehicle after tumor inoculation. Mice injected with Seraphina-transfected clones 1 and 2 cells but not Seraphina wild-type or cells transfected with the empty vector presented a statistically significant prolonged OS after treatment with doxorubicin compared with vehicle-treated recipients. (F) Follow-up studies of tumor metabolic activity by micro-PET performed 2 weeks after initiation of therapy revealed a better response after treatment in Seraphina clone 1 recipients than in clone 2 transplanted mice, whereas no response was observed in control mice carrying BL cells transfected with empty p-MIRG or parental wild-type cells.

and vehicle-treated subgroups. Conversely, mice injected with clones 1 and 2 receiving doxorubicin presented longer OS compared with vehicle-treated recipients, these differences being more pronounced for mice carrying clone 2-derived lymphomas (median OS, 32 vs 22 days; $P < .001$) than for those with clone 1 (29 vs 25 days, $P = .01$; Figure 3E). Accordingly, reduction of lymphoma volumes and decreased glycolytic tumor activities were observed in mouse recipients transplanted with clones 1 and 2 cells compared with control mice, as determined by PET imaging studies (Figure 3F). These data indicate that sensitivity to doxorubicin is correlated with *BIM* expression in BL xenografts in vivo, therefore expanding our previous observations in vitro.

BIM regulates chemoresistance in lymphomas developed in Eμ-*MYC* and *BIM*-deficient mice

A previous study demonstrated that *BIM*-mutant Eμ-*MYC* transgenic mice developed B-cell leukemias and lymphomas more efficiently than Eμ-*MYC* transgenes.[24] We used this validated model to test whether *BIM* could condition sensitivity to chemotherapy in mouse $B220^+IgM^+$ B-cell lymphomas (Figure 4A; supplemental Figure 5). Western blot analysis revealed a reduction in *BIM* expression levels in Eμ-*MYC*-*BIM*$^{+/-}$ lymphomas compared with Eμ-*MYC* lymphomas (Figure 4B). Then, mature $B220^+IgM^+$ tumor lymphocytes were isolated from Eμ-*MYC* or in Eμ-*MYC*-*BIM*$^{+/-}$ transgenes and treated with doxorubicin ex vivo. Eμ-*MYC* lymphoma cells showed decreased survival and higher apoptotic levels than Eμ-*MYC*-*BIM*$^{+/-}$ lymphomas after doxorubicin treatment (Figure 4C). To test this observation in vivo, 2.5×10^6 mature $B220^+IgM^+$ tumor lymphocytes isolated from 6 different lymphomas developed in Eμ-*MYC* or in Eμ-*MYC*-*BIM*$^{+/-}$ transgenes were injected intravenously into RAG2$^{-/-}\gamma c^{-/-}$ recipients (supplemental Table 3). One week after inoculation, doxorubicin versus vehicle (PBS) was administered (Figure 4D). After treatment and compared with vehicle-treated mice, mice carrying Eμ-*MYC* lymphomas presented an extended survival time of 30 days (median OS, 20 vs 50 days; $P = .001$), whereas those with Eμ-*MYC*-*BIM*$^{+/-}$ lymphomas only extended survival in 3 days (median OS, 43 vs 46 days; $P = .03$; Figure 4E). Thus, Eμ-*MYC*-*BIM*$^{+/-}$ lymphomas were more resistant to chemotherapy than Eμ-*MYC* lymphomas in vivo. Accordingly, at day 100 after injection, 4 Eμ-*MYC* mouse recipients remained disease-free versus only 2 in the Eμ-*MYC*-*BIM*$^{+/-}$ subgroup. In agreement with these data, PET studies showed a marked reduction in the glycolytic tumor activity in Eμ-*MYC* lymphoma recipients compared with mice with Eμ-*MYC*-*BIM*$^{+/-}$ lymphomas after doxorubicin treatment (Figure 4F). These data confirm our previous results in a different mouse model, reinforcing the concept that *BIM* expression levels modulate chemosensitivity in *MYC*-driven lymphomas.

BL chemoresistance can be overcome by pharmacologic reexpression of BIM

Last, to begin to translate these findings to the clinic, we tested whether resistance to chemotherapy was reversible on pharmacologic induction of BIM expression in BL-resistant lymphomas. Treatment of *BIM* epigenetically silenced cell lines with 5-Aza induced a 1.5- to 2.5-fold up-regulation of *BIM* expression, whereas treatment with vorinostat resulted in a 3.5- to 4-fold *BIM* reexpression (Figure 1G). Induction of BIM in BL cells was associated with a partial reversion of the resistance to doxorubicin in vitro, along with an increase in the apoptotic rates, which were more pronounced for vorinostat than for 5-Aza (Figure 5A). However, no differences in cell viability or apoptotic rates were observed after vorinostat and doxorubicin therapy in the *BIM* unmethylated cell lines (Figure 5B). We therefore selected vorinostat to explore whether similar results could be observed in vivo. Thus, 2.5×10^6 cells from the wild-type Seraphina cell line (with complete *BIM* hypermethylation) were intravenously inoculated into 5 RAG2$^{-/-}\gamma c^{-/-}$ mouse cohorts (including 10-15 mice on each), which received treatment with vorinostat, doxorubicin, vorinostat plus doxorubicin, vorinostat plus doxorubicin plus cyclophosphamide, or vehicle (DMSO). Vorinostat was administered at low doses, enough to induce BIM expression without killing the lymphoma cells in vitro (Figure 5A-B; and data not shown). Mice treated with DMSO presented similar survival duration as the vorinostat-treated and doxorubicin-treated subgroups (median OS, 35 vs 36 vs 33 days, respectively; $P = .9$). Mice treated with vorinostat plus doxorubicin presented longer OS compared with control mice (median OS, 45 vs 33 days; $P = .005$). These results confirm our previous observations and further indicate that BIM reexpression may reverse chemoresistance to doxorubicin in vivo. Next we tested cyclophosphamide, a drug that is not active in vitro as it requires hepatic activation in vivo.[32] Notably, a longer OS was observed in mice treated with vorinostat, doxorubicin, and cyclophosphamide compared with doxorubicin- and vorinostat-treated mice (median OS, not reached vs 45 days; $P < .001$). Indeed, 5 of 10 mice treated with the triple combination remained alive and free of disease at day 150 after injection (Figure 5C; supplemental Figure 6). Treatment of tumors with vorinostat plus chemotherapy was associated with higher apoptotic rates, decreased cell growth, and activation of the intrinsic apoptotic pathway (Figure 5D-E). In addition, monitoring of tumor responses using PET imaging showed a marked reduction in tumor volume and glycolytic activity in mice treated with vorinostat and chemotherapy compared with control mice (Figure 5F). These data indicate that the combination of vorinostat at low doses (which allows reexpression of BIM, thus sensitizing cells to chemotherapy) followed by doxorubicin and cyclophosphamide was the optimal therapeutic in the xenograft model, as it reversed chemotherapeutic resistance and significantly increased survival of mice.

Discussion

Our study demonstrates the power of coupling clinical investigation with experimental research to deal with a medical problem. We have used different in vitro assays and in vivo studies in human BL xenografts and in transgenic mice to show that the epigenetic silencing of BIM is a critical mechanism of chemotherapy resistance in MYC-driven lymphomas. Accordingly, therapies that reactivate BIM expression, such as vorinostat, can reverse chemoresistance and enhance the efficacy of doxorubicin and cyclophosphamide therapy in BL. Other studies aiming to evaluate the apoptosis and therapeutic activities of HDACis have been conducted in similar mouse models of lymphoma.[33,34] These and our report underline the importance of using appropriate experimental animal models for the preclinical evaluation of novel therapeutic agents, aiming to select optimal drug combinations to treat human disease.

BIM plays a central role in the therapeutic resistance of some solid tumors and myeloid leukemias, whereby BIM inactivation is caused by selective phosphorylation that targets it for degradation in the proteasome.[19-23] This post-transcriptional BIM inactivation mediated therapeutic resistance to tyrosine-kinase inhibitors in

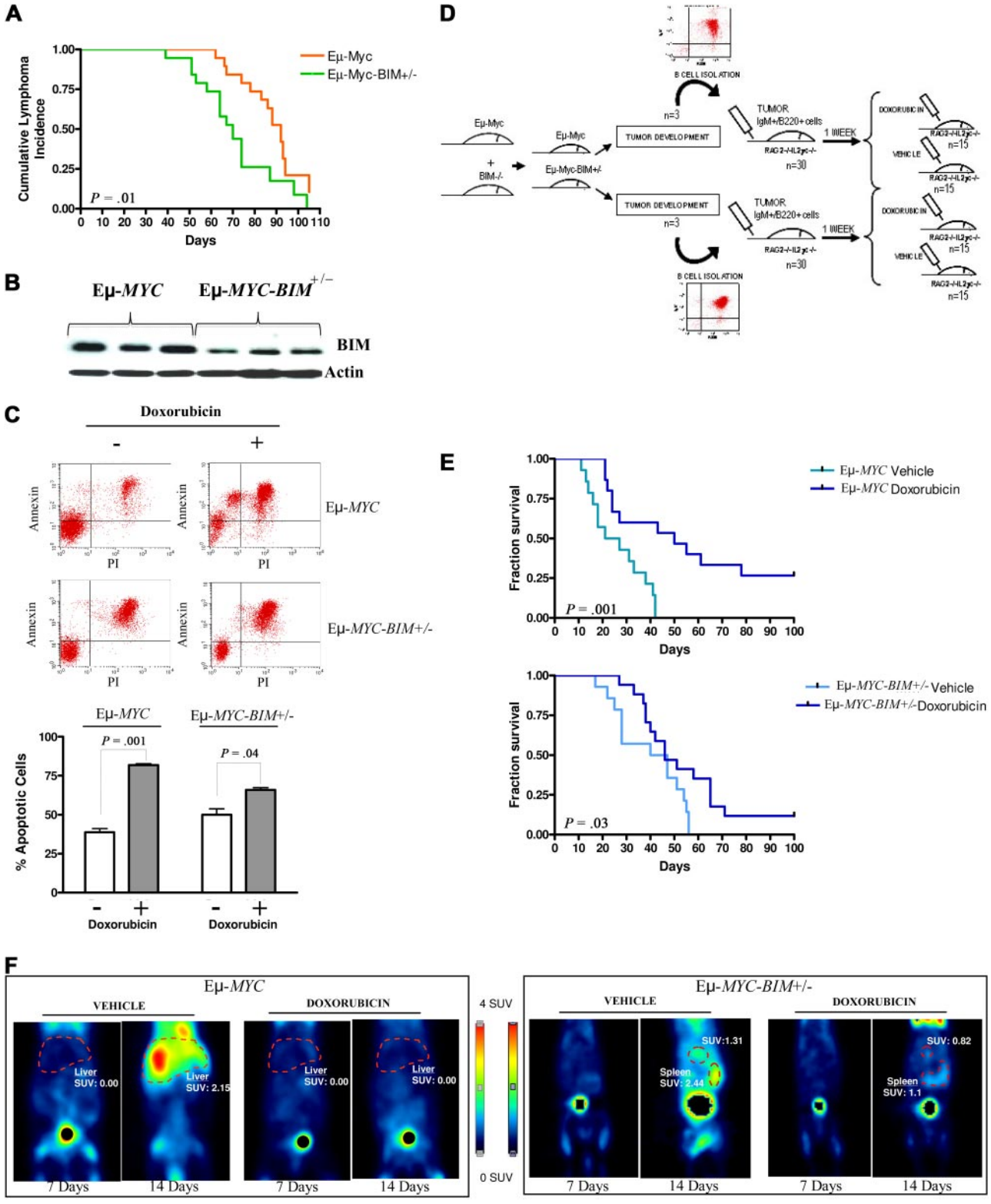

Figure 4. Lymphoma characterization, B-cell isolation, and therapy of double *Eμ-Myc*- and *BIM*-deficient transgenic mice. (A) Kaplan-Meier survival curves for *Eμ-MYC* and *Eμ-Myc-BIM*$^{+/-}$ mice. (B) Determination of BIM protein expression levels in B220^{+}IgM^{+} mature *Eμ-MYC* and *Eμ-Myc-BIM*$^{+/-}$ lymphomas by Western blot analysis. (C) Mature B220^{+}IgM^{+} tumor lymphocytes isolated from *Eμ-MYC* and *Eμ-Myc-BIM*$^{+/-}$ mice were BCR-activated with anti-IgM and treated with doxorubicin. *Eμ-Myc* B220^{+}IgM^{+} lymphoma cells showed decreased survival and higher apoptotic levels than *Eμ-Myc-BIM*$^{+/-}$ B220^{+}IgM^{+} lymphoma cells, according to annexin V/fluorescein isothiocyanate staining. (D) Representative diagram of the experimental therapeutic design to test whether *Eμ-MYC* lymphoma cells were more sensitive than *Eμ-MYC-BIM*$^{+/-}$ lymphoma cells to doxorubicin treatment in vivo. (E) Kaplan-Meier survival curves for mice transplanted with mature B-cell *Eμ-Myc* and *Eμ-Myc-BIM*$^{+/-}$ lymphoma cells treated with doxorubicin versus vehicle. Compared with DMSO-treated mouse recipients, mice carrying *Eμ-Myc* lymphomas presented longer survival after therapy than those with *Eμ-Myc-BIM*$^{+/-}$ lymphomas. (F) Micro-PET studies showed a significant reduction in the glycolytic tumor activity in *Eμ-Myc* lymphoma recipients compared with mice with *Eμ-Myc-BIM*$^{+/-}$ lymphomas. PET studies were performed at day 7 (just before initiation of therapy) and at day 14 (1 week after therapy).

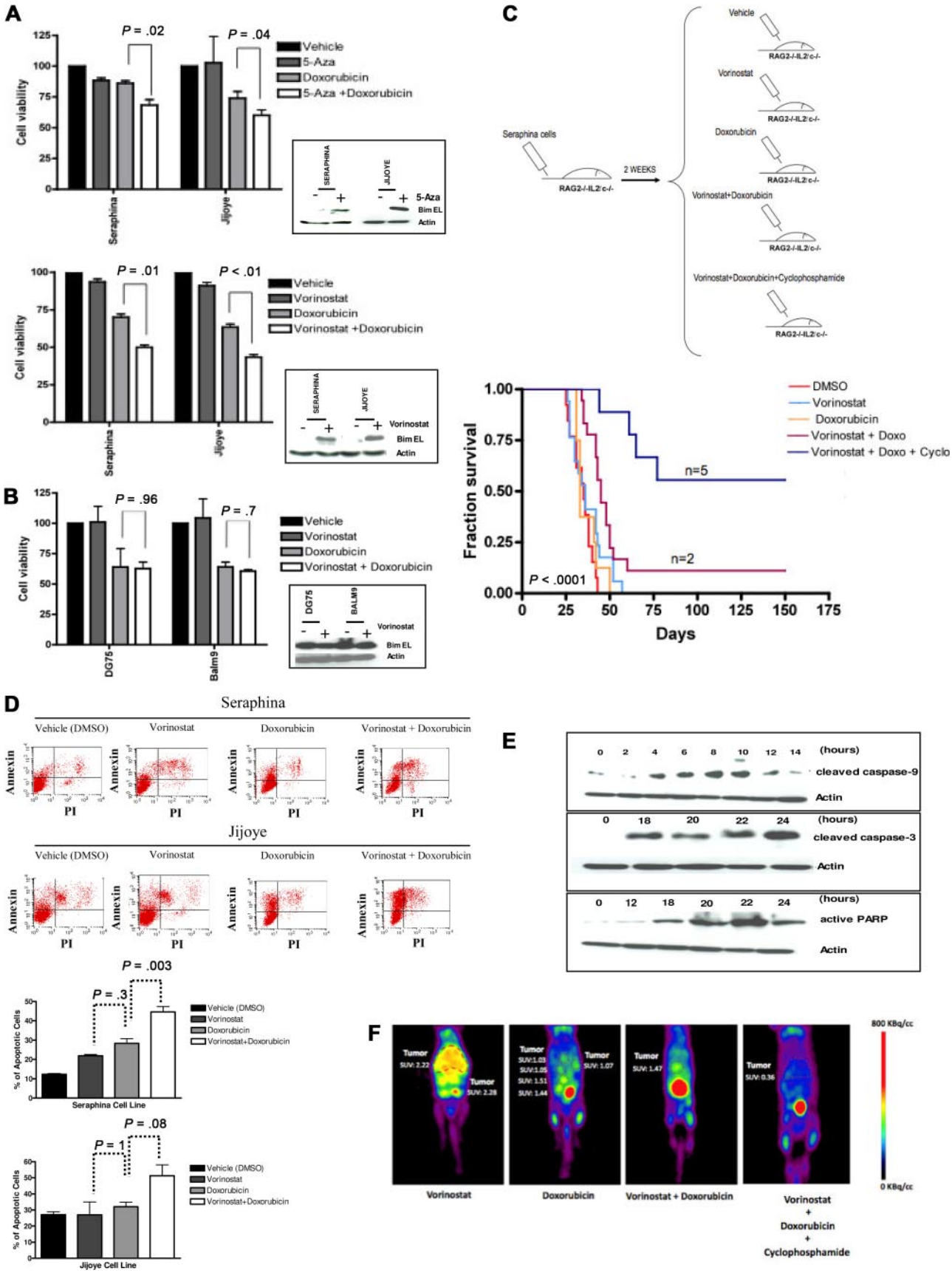

Figure 5.

lung cancer,[35] MEK inhibitors in melanomas,[36] paclitaxel in epithelial tumors,[19] imatimib in chronic myeloid leukemia,[20] and sorafenib (a *RAF* kinase inhibitor) in acute myeloid leukemia.[37] Restoration of *BIM* expression with the proteasome inhibitor bortezomib or by mimicking its function with the BH3-mimetic ABT-737 reversed tumor chemoresistance.[19,20,35-37] Herein, we confirm the critical role of BIM in regulating chemoresistance but, different from these reports, BIM inactivation in BL cells occurred at the transcriptional level and not post-transcriptionally. This observation may be of clinical relevance, as the reactivation of BIM function aiming to bypass chemoresistance can be achieved with different treatment modalities. Thus, in BL cells with *BIM* epigenetic silencing, therapies such as demethylating agents or HDACis can restore *BIM* expression and reverse chemoresistance. Conversely, in most other leukemias and solid tumors, BIM post-transcriptional modifications can be repaired with bortezomib or with ABT-737, thus sensitizing cells to chemotherapy. Together, our data indicate that the combination of HDACis and high-dose chemotherapy may overcome chemoresistance, achieve durable remission and improve survival of patients with BL.

Vorinostat as a single agent was approved by the Food and Drug Administration in October 2006 for the treatment of progressive, persistent, or recurrent cutaneous T-cell lymphoma (CTCL) after 2 prior systemic therapies, achieving clinical effective responses with an acceptable safety profile.[38] More recently, the HDACi romidepsin (FK-228) has been also approved by the Food and Drug Administration for the treatment of CTCL patients who have received at least 1 prior systemic therapy.[39] In addition, other HDACis, such as panobinostat (LBH589), belinostat (PXD101), and miocetinostat (MGCD0103), have demonstrated therapeutic potential as monotherapy or in combination with other antitumor drugs in CTCLs and in other hematologic malignancies.[40] Indeed, at least 80 clinical trials with more than 10 different HDACis are underway, testing these compounds in leukemias, lymphomas, myeloma, and solid tumors.[41] Besides vorinostat, we have recently evaluated the therapeutic efficacy of other different HDCAis in combination with doxorubicin in our BL cellular models in vitro, obtaining rather similar results in terms of BIM reactivation and of reversion of chemoresistance (data not shown). Our current goal is to identify the HDACi that, in combination with doxorubicin and cyclophosphamide, shows the best therapeutic activity with minor toxicity in our preclinical BL mouse models. Once the optimal combination therapy has been defined, we expect to design a clinical trial to evaluate the maximum tolerated dose and the therapeutic efficacy of the combination of the selected HDACi with rituximab and HyperCVAD in adult patients with refractory or early relapsed BL.

Acknowledgments

The authors thank Drs Martin Dyer (University of Leicester, Leicester, United Kingdom), William Harrington (University of Miami, Miami, FL), and James Stone (University of Alberta, Edmonton, AB) for providing cell lines, Drs Maria Collantes and Iván Peñuelas (University of Navarra) for mouse imaging studies, Dr Marta García-Granero (University of Navarra) for support with the statistical studies, Izaskun Sesma for excellent technical work with mice, Merck Sharp & Dohme (Spain) for providing vorinostat, and Drs Martin Dyer and Reiner Siebert (Kiel University, Germany) for their helpful comments during the preparation of this manuscript.

This work was supported by the Spanish Ministry of Science and Innovation (grants PI081878 and RTICC-RD06/0020-0088/0111/0066/0006)-FEDER, the Navarra Government (Education and Health Councils), the Cooperación de Investigación Transpirenaica en la Terapia Innovadora de la Leucemia (CITTIL) Spanish-French EU Program, and the UTE-Center for Applied Medical Research project. J.A.R.-L. and E.B. are supported by predoctoral fellowships from the Spanish Ministry of Science and Innovation.

Authorship

Contribution: J.A.R.-L. designed the study, performed most of the experiments, analyzed and interpreted the data, and contributed to manuscript writing; E.F.R., V.F., E.B., A.J.R., X.A., and J.A.R. performed research and analyzed and interpreted data; M.J.C., C.P., and J.M.H. contributed samples and performed research; J.R.-G. contributed samples, performed research, and analyzed and interpreted data; F.P. contributed samples and analyzed and interpreted data; and J.A.M.-C. designed the study, analyzed and interpreted data, and wrote the manuscript.

Conflict-of-interest disclosure: The authors declare no competing financial interests.

Correspondence: Jose A. Martinez-Climent, Division of Oncology, Center for Applied Medical Research, University of Navarra, Avda Pio XII, 55, Pamplona 31008, Spain; e-mail: jamcliment@unav.es.

References

1. Jaffe ES, Harris NL, Stein H, Isaacson PG. Classification of lymphoid neoplasms: the microscope as a tool for disease discovery. *Blood.* 2008; 112(12):4384-4399.
2. Harris NL, Jaffe ES, Diebold J, et al. The World Health Organization classification of neoplasms of the hematopoietic and lymphoid tissues: report of the Clinical Advisory Committee meeting–Airlie House, Virginia, November, 1997. *Hematol J.* 2000;1(1):53-66.
3. Taub R, Kirsch I, Morton C, et al. Translocation of the c-myc gene into the immunoglobulin heavy chain locus in human Burkitt lymphoma and murine plasmacytoma cells. *Proc Natl Acad Sci U S A.* 1982;79(24):7837-7841.

Figure 5. Resistance to doxorubicin is reversible on treatment with HDACis in human BL-xenografted mice. (A) Treatment of BL cells with 5-Aza or vorinostat resulted in BIM reexpression (Figure 1E). Subsequent incubation of these cells with doxorubicin led to a higher decrease in cell viability in Seraphina and Jijoye cells treated with vorinostat versus 5-Aza therapy. (B) Treatment of the BL unmethylated cell lines Balm9 and DG75 with vorinostat did not increase BIM expression. In addition, no differences in cell viability were observed between doxorubicin and doxorubicin plus vorinostat therapies in these cells. (C) Experimental design and Kaplan-Meier survival curves for 5 mouse cohorts transplanted with Seraphina cells with *BIM* hypermethylation and treated with vehicle (DMSO), low-dose vorinostat, doxorubicin, low-dose vorinostat plus doxorubicin, and low-dose vorinostat plus doxorubicin and cyclophosphamide. Those receiving the combination of low-dose vorinostat plus doxorubicin and cyclophosphamide resulted in the longest OS compared with the other subgroups. (D) An increase in the apoptotic rates was observed on treatment with vorinostat and doxorubicin in Seraphina and Jijoye cells compared with other in vitro treatments, as determined by annexin V/propidium iodide staining. (E) Representative study of the induction of apoptosis in Seraphina cells after treatment with vorinostat plus doxorubicin, as shown by caspase 3 and 9 activation and increased PARP expression. (F) Micro-PET studies showed that mice treated with vorinostat plus doxorubicin and with vorinostat plus doxorubicin and cyclophosphamide presented a significant decrease in tumor activity compared with mice treated with single vorinostat or doxorubicin, which was correlated with prolonged survival. Images were taken 2 weeks after treatment with the corresponding compound.

4. Gelmann EP, Psallidopoulos MC, Papas TS, Dalla-Favera R. Identification of reciprocal translocation sites within the c-myc oncogene and immunoglobulin mu locus in a Burkitt lymphoma. *Nature.* 1983;306(5945):799-803.
5. Blum KA, Lozanski G, Byrd JC. Adult Burkitt leukemia and lymphoma. *Blood.* 2004;104(10):3009-3020.
6. Yustein JT, Dang CV. Biology and treatment of Burkitt's lymphoma. *Curr Opin Hematol.* 2007; 14(4):375-381.
7. Garcia JL, Hernandez JM, Gutierrez NC, et al. Abnormalities on 1q and 7q are associated with poor outcome in sporadic Burkitt's lymphoma: a cytogenetic and comparative genomic hybridization study. *Leukemia.* 2003;17(10):2016-2024.
8. Murphy SB, Fairclough DL, Hutchison RE, Berard CW. Non-Hodgkin's lymphomas of childhood: an analysis of the histology, staging, and response to treatment of 338 cases at a single institution. *J Clin Oncol.* 1989;7(2):186-193.
9. Hummel M, Bentink S, Berger H, et al. A biologic definition of Burkitt's lymphoma from transcriptional and genomic profiling. *N Engl J Med.* 2006; 354(23):2419-2430.
10. Dave SS, Fu K, Wright GW, et al. Molecular diagnosis of Burkitt's lymphoma. *N Engl J Med.* 2006; 354(23):2431-2442.
11. Levine AM. Challenges in the management of Burkitt's lymphoma. *Clin Lymphoma.* 2002; 3(suppl 1):S19-S25.
12. Bociek RG. Adult Burkitt's lymphoma. *Clin Lymphoma.* 2005;6(1):11-20.
13. Griffin TC, Weitzman S, Weinstein H, et al. A study of rituximab and ifosfamide, carboplatin, and etoposide chemotherapy in children with recurrent/refractory B-cell (CD20+) non-Hodgkin lymphoma and mature B-cell acute lymphoblastic leukemia: a report from the Children's Oncology Group. *Pediatr Blood Cancer.* 2009;52(2):177-181.
14. Gutierrez MI, Cherney B, Hussain A, et al. Bax is frequently compromised in Burkitt's lymphomas with irreversible resistance to Fas-induced apoptosis. *Cancer Res.* 1999;59(3):696-703.
15. Valnet-Rabier MB, Challier B, Thiebault S, et al. c-Flip protein expression in Burkitt's lymphomas is associated with a poor clinical outcome. *Br J Haematol.* 2005;128(6):767-773.
16. Tafuku S, Matsuda T, Kawakami H, Tomita M, Yagita H, Mori N. Potential mechanism of resistance to TRAIL-induced apoptosis in Burkitt's lymphoma. *Eur J Haematol.* 2006;76(1):64-74.
17. Nomura Y, Yoshida S, Karube K, et al. Estimation of the relationship between caspase-3 expression and clinical outcome of Burkitt's and Burkitt-like lymphoma. *Cancer Sci.* 2008;99(8):1564-1569.
18. Mestre-Escorihuela C, Rubio-Moscardo F, Richter JA, et al. Homozygous deletions localize novel tumor suppressor genes in B-cell lymphomas. *Blood.* 2007;109(1):271-280.
19. Tan TT, Degenhardt K, Nelson DA, et al. Key roles of BIM-driven apoptosis in epithelial tumors and rational chemotherapy. *Cancer Cell.* 2005; 7(3):227-238.
20. Kuroda J, Puthalakath H, Cragg MS, et al. Bim and Bad mediate imatinib-induced killing of Bcr/Abl+ leukemic cells, and resistance due to their loss is overcome by a BH3 mimetic. *Proc Natl Acad Sci U S A.* 2006;103(40):14907-14912.
21. Bouillet P, Metcalf D, Huang DC, et al. Proapoptotic Bcl-2 relative Bim required for certain apoptotic responses, leukocyte homeostasis, and to preclude autoimmunity. *Science.* 1999; 286(5445):1735-1738.
22. Bouillet P, Purton JF, Godfrey DI, et al. BH3-only Bcl-2 family member Bim is required for apoptosis of autoreactive thymocytes. *Nature.* 2002;415(6874): 922-926.
23. Enders A, Bouillet P, Puthalakath H, Xu Y, Tarlinton DM, Strasser A. Loss of the pro-apoptotic BH3-only Bcl-2 family member Bim inhibits BCR stimulation-induced apoptosis and deletion of autoreactive B cells. *J Exp Med.* 2003;198(7): 1119-1126.
24. Egle A, Harris AW, Bouillet P, Cory S. Bim is a suppressor of Myc-induced mouse B cell leukemia. *Proc Natl Acad Sci U S A.* 2004;101(16): 6164-6169.
25. Hemann MT, Bric A, Teruya-Feldstein J, et al. Evasion of the p53 tumour surveillance network by tumour-derived MYC mutants. *Nature.* 2005; 436(7052):807-811.
26. Sanchez-Izquierdo D, Siebert R, Harder L, et al. Detection of translocations affecting the BCL6 locus in B cell non-Hodgkin's lymphoma by interphase fluorescence in situ hybridization. *Leukemia.* 2001;15(9):1475-1484.
27. Oriol A, Ribera JM, Bergua J, et al. High-dose chemotherapy and immunotherapy in adult Burkitt lymphoma: comparison of results in human immunodeficiency virus-infected and noninfected patients. *Cancer.* 2008;113(1):117-125.
28. Roman-Gomez J, Cordeu L, Agirre X, et al. Epigenetic regulation of Wnt-signaling pathway in acute lymphoblastic leukemia. *Blood.* 2007; 109(8):3462-3469.
29. Rubio-Moscardo F, Blesa D, Mestre C, et al. Characterization of 8p21.3 chromosomal deletions in B-cell lymphoma: TRAIL-R1 and TRAIL-R2 as candidate dosage-dependent tumor suppressor genes. *Blood.* 2005;106(9):3214-3222.
30. Traggiai E, Chicha L, Mazzucchelli L, et al. Development of a human adaptive immune system in cord blood cell-transplanted mice. *Science.* 2004; 304(5667):104-107.
31. Bhatia K, Huppi K, Spangler G, Siwarski D, Iyer R, Magrath I. Point mutations in the c-Myc transactivation domain are common in Burkitt's lymphoma and mouse plasmacytomas. *Nat Genet.* 1993;5(1):56-61.
32. de Jonge ME, Huitema AD, Rodenhuis S, Beijnen JH. Clinical pharmacokinetics of cyclophosphamide. *Clin Pharmacokinet.* 2005;44(11):1135-1164.
33. Lindemann RK, Newbold A, Whitecross KF, et al. Analysis of the apoptotic and therapeutic activities of histone deacetylase inhibitors by using a mouse model of B cell lymphoma. *Proc Natl Acad Sci U S A.* 2007;104(19):8071-8076.
34. Frew AJ, Lindemann RK, Martin BP, et al. Combination therapy of established cancer using a histone deacetylase inhibitor and a TRAIL receptor agonist. *Proc Natl Acad Sci U S A.* 2008;105(32): 11317-11322.
35. Cragg MS, Kuroda J, Puthalakath H, Huang DC, Strasser A. Gefitinib-induced killing of NSCLC cell lines expressing mutant EGFR requires BIM and can be enhanced by BH3 mimetics. *PLoS Med.* 2007;4(10):1681-1689; discussion 1690.
36. Cragg MS, Jansen ES, Cook M, Harris C, Strasser A, Scott CL. Treatment of B-RAF mutant human tumor cells with a MEK inhibitor requires Bim and is enhanced by a BH3 mimetic. *J Clin Invest.* 2008;118(11):3651-3659.
37. Zhang W, Konopleva M, Ruvolo VR, et al. Sorafenib induces apoptosis of AML cells via Bim-mediated activation of the intrinsic apoptotic pathway. *Leukemia.* 2008;22(4):808-818.
38. Olsen EA, Kim YH, Kuzel TM, et al. Phase IIb multicenter trial of vorinostat in patients with persistent, progressive, or treatment refractory cutaneous T-cell lymphoma. *J Clin Oncol.* 2007; 25(21):3109-3115.
39. Piekarz RL, Frye R, Turner M, et al. Phase II multi-institutional trial of the histone deacetylase inhibitor romidepsin as monotherapy for patients with cutaneous T-cell lymphoma. *J Clin Oncol.* 2009;27(32):5410-5417.
40. Gupta M, Ansell SM, Novak AJ, Kumar S, Kaufmann SH, Witzig TE. Inhibition of histone deacetylase overcomes rapamycin-mediated resistance in diffuse large B-cell lymphoma by inhibiting Akt signaling through mTORC2. *Blood.* 2009;114(14):2926-2935.
41. Tan J, Cang S, Ma Y, Petrillo RL, Liu D. Novel histone deacetylase inhibitors in clinical trials as anti-cancer agents. *J Hematol Oncol.* 2010;3:5.
42. Richter JA, Rullan A, Beltran E, et al. Epigentic silencing of BIM mediates chemotherapy resistance of patients with Burkitt lymphoma that can be overcome by therapeutic reactivation of BIM in mouse and human lymphoma models [abstract]. *Blood.* 2008;112(11):227. Abstract 607.